# Can we improve the representation of modelled ocean mixed-layer by assimilating surface-only satellite-derived data? A case study for the tropical Pacific during the 1997-98 El Nino

Fabien Durand, Lionel Gourdeau, Jacques Verron, Thierry Delcroix

# Can we improve the representation of modeled ocean mixed layer by assimilating surface-only satellite-derived data? A case study for the tropical Pacific during the 1997–1998 El Niño

Fabien Durand, Lionel Gourdeau, and Thierry Delcroix

Laboratoire d'Etudes en Géophysique et Océanographie Spatiales (LEGOS)/Institut de Recherché Pour le Développement (IRD), Toulouse, France

Jacques Verron

Laboratoire des Ecoulements Géophysiques et Industriels (LEGI), CNRS, Grenoble, France

Received 17 February 2003; accepted 12 March 2003; published 24 June 2003.

[1] In the tropical oceans the density mixed layer does influence the ocean-atmosphere interactions, a feature that is fundamental to the development of energetic climatic events such as the El Niño-Southern Oscillation (ENSO) phenomenon. The aim of this work is to take advantage of existing sea surface temperature (SST) and velocity together with future sea surface salinity (SSS) satellite-derived data by assimilating these data in a primitive equation model in order to improve the modeled mixed layer. As satellite SSS data are not yet available, and to better analyze how assimilation works, we performed twin experiments in a context that renders assimilation conclusive with regard to real experiment. Two simulations using different forcing were used for the experiments. They have errors that are comparable to the ones between any simulation and real observations. The assimilation scheme is an adaptive version of the SEEK filter [*Pham et al.*, 1998] readily usable for assimilating real data. An assimilation experiment was conducted covering the 1997–1998 ENSO event to analyze the main characteristics of the actual mixed layer. Looking in particular at the relevance of SSS, SST, mixed layer depth, and barrier layer thickness, satellite-derived data prove to be useful to better simulate the oceanic mixed layer. Velocity data are specially needed to control the zonal equatorial current. Interestingly, assimilation of surface-only data still worked well below the mixed layer, and some improvements were detectable in terms of barrier layer thickness, even though the limit of the assimilation scheme was reached. *INDEX TERMS:* 4522 Oceanography: Physical: El Niño; 3260 Mathematical Geophysics: Inverse theory; 4231 Oceanography: General: Equatorial oceanography; 4215 Oceanography: General: Climate and interannual variability (3309); *KEYWORDS:* data assimilation, tropical Pacific, mixed layer

**Citation:** Durand, F., L. Gourdeau, T. Delcroix, and J. Verron, Can we improve the representation of modeled ocean mixed layer by assimilating surface-only satellite-derived data? A case study for the tropical Pacific during the 1997–1998 El Niño, *J. Geophys. Res.*, *108*(C6), 3200, doi:10.1029/2002JC001603, 2003.

## 1. Introduction

[2] The density mixed layer (in this paper, only the oceanic mixed layer is considered), i.e., the interface between the atmosphere and the underlying inner ocean, is characterized by quasi-homogenous temperature and salinity throughout its thickness. Its dynamics is conditioned both by the atmospheric fluxes (heat, freshwater and momentum) at the surface and by the subsurface ocean dynamics. The mixed layer is a key component of the climatic system. In the tropics, large-scale atmospheric convection develops mostly above the critical threshold of 29°C in sea surface temperature (SST), and in the western Pacific, the warm pool area (SST > 29°C) is fundamental to the development of El Niño-Southern Oscillation (ENSO) [e.g., *Gill*, 1983; *Fu et al.*, 1986; *Picaut and Delcroix*, 1995]. In the equatorial oceans, whereas the SST field has long been identified as a key parameter for the driving of the atmosphere, near-surface salinity is now considered to play a significant role in the ocean dynamics and thermodynamics as well as in influencing exchanges between ocean and atmosphere. Notably, a salt-stratified barrier layer may exist within the isothermal layer located above the thermocline [*Lukas and Lindstrom*, 1991]. This barrier layer may reduce drastically the depth of the density mixed layer, and isolate it from the subsurface, rendering it very reactive to the atmospheric forcing. The existence or absence of such a barrier layer is suspected to have a strong influence on the development of ENSO events in the tropical Pacific [*Vialard and Delecluse*, 1998; *Lengaigne et al.*, 2002; *Maes et al.*, 2002].


0148-0227/03/2002JC001603

[3] Despite enormous progress in the last decade [*Stockdale et al.*, 1998; *Delecluse et al.*, 1998], ocean numerical models still have difficulties in properly simulating the mixed layer structure, notably on account of the approximate representation of physical processes involved in its dynamics, and of the erroneous atmospheric boundary conditions applied. However, a stringent test of the quality of any numerical simulation of the tropical ocean aiming at understanding the relevant oceanic dynamical processes, or forecasting the time evolution of the coupled climatic system, is its capability to simulate accurately the upper ocean thermohaline structure. A well-known deficiency of ocean models is their tendency to produce spurious drifts in both SST and sea surface salinity (SSS) fields. In order to control these drifts, a prevailing makeshift solution consists of introducing correction terms in the model equations, typically in the form of a relaxation toward observed SST and SSS fields. Another solution consists of estimating an ad hoc correction of the systematic biases of the forcing fluxes based on the relaxation term, and to run the model with the corrected forcing fluxes [*Vialard et al.*, 2001, 2002]. Neither of these two kinds of solutions can be entirely satisfactory. Indeed, although global coverage high-frequency SST observations have become available [*Reynolds and Smith*, 1994], one is compelled to rely on climatological fields [e.g., *Levitus et al.*, 1994] for SSS relaxation. These solutions also suffer from the very crude relaxation method used [*Reynolds et al.*, 1998; *Durand et al.*, 2002 (hereinafter referred to as D02)].

[4] One way to improve simulations of the mixed layer is to obtain better observations of atmospheric fluxes. Great efforts are being made in this direction, but there is still a long way to go before observed, good quality atmospheric forcing fluxes become available to ocean modelers. As for the atmospheric reanalysis products released in the last few years [*Kalnay et al.*, 1996; *Gibson et al.*, 1997], they still suffer from high uncertainties (see section 2). One could think of using coupled ocean-atmosphere simulations to get rid of the problem of ocean model forcing since theoretically, a coupled model ensures consistency between the oceanic mixed layer structure simulated and the ocean-atmosphere fluxes. However, once again we have to deal with the drawbacks inherent to numerical tools. Another way is to draw upon the huge progress made during the last two decades with regards to ocean surface remote sensing. We are now on the verge of observing satisfactorily at synoptic scales all the relevant oceanic surface fields by satellite, and notably: a) sea level variability, now accurately monitored by satellite altimetry (TOPEX/Poseidon and Jason), which can be used, in addition to wind stress and SST fields, to estimate surface currents variability with high accuracy [*Bonjean and Lagerloef*, 2002], and b) good quality global coverage high-resolution SST observations available for more than 15 years (see http://podaac.jpl.nasa.gov/sst/). In addition, satellite missions to be launched in the near future are expected to provide SSS measurements [*Font et al.*, 2000; *Lagerloef and Delcroix*, 2001]. All these data sets bring complementary information: altimetric sea level is a good proxy for the thermohaline variability at depth, particularly in the tropical oceans, whereas SST and SSS are intimately linked to the mixed layer dynamics.

[5] Motivated by the role of the mixed layer in the ocean/atmosphere processes and its influence on predictive skill from ocean/atmosphere coupled models, the objective of this paper is to take advantage of the expected SSS satellite data in conjunction with the currently available SST and surface current satellite data to improve the modeling of the oceanic mixed layer, making use of an advanced data assimilation system. Knowing the importance of tropical oceans, especially the tropical Pacific, in the climate system, and the presumably acceptable level of accuracy of future satellite-derived SSS measurements in the tropical areas, we focused our experiment on the tropical Pacific.

[6] Great efforts have been devoted to constraining the modeled subsurface structure (typically: the thermocline in the tropical oceans) by data assimilation, using mainly altimetric sea level data and in situ temperature profiles [e.g., *Fukumori et al.*, 1999; *Gourdeau et al.*, 2000; *Weaver et al.*, 2002]. By contrast, very few assimilation studies have been conducted to tackle the issue of the control of the mixed layer. Some authors have proven both the interest and the feasibility of SST data assimilation to improve ocean numerical modeling [*Deltel*, 2002; *Testut et al.*, 2003; *Andreu Burillo*, 2002]. The impact of SSS satellite data on the dynamics simulated by an Ocean General Circulation Model (OGCM) was analyzed through an assimilation method, called the SEEK filter [*Pham et al.*, 1998], in the context of ''academic'' twin experiments in D02,. Basically, the SEEK filter consists of a reduced order Kalman filter, which performs sequential corrections along a limited set of error modes which are called the reduced basis. By ''academic'' twin experiments, we mean that assimilation is used in optimal conditions where all the theoretical prerequisites are fulfilled. In particular, the analysis in D02 is limited to assimilation experiments in which the reduced basis used for the assimilation is consistent with the new information brought by the observations (the innovation sequence). Results indicate that the assimilation of SSS data using such a sophisticated assimilation technique accurately constrains most of the model variables throughout the whole upper ocean. These experiments were a first step toward the use of more realistic data. They provide an upper limit of SSS assimilation performance, but they remain rather too far from reality to be straightforwardly extrapolated to a real case. In the absence of actual SSS synoptic data, this paper deals with more realistic twin experiments.

[7] The present work is novel in the sense that it considers jointly a variety of satellite-derived data (SST, SSS, and surface currents as inferred from altimetry and surface wind fields). As in D02, the study is based on classical Observing System Simulation Experiments (OSSEs). The realism of the experiments conducted was always present in our mind. In particular, any realistic assimilation experiment requires taking into account the discrepancies that can exist between the modeled and observed variables both in terms of bias and variability. This led us to the implementation of an adaptive version of the SEEK filter. For this purpose, we used two interannual simulations of the tropical Pacific Ocean forced by different atmospheric products. This set of runs is described in section 2. The assimilation scheme and the twin experiments conducted in order to control the mixed layer by using SSS, SST and surface current data are presented in section 3. We then assessed the effectiveness of

the assimilation from a statistical (section 4) and physical (section 5) point of view. Section 6 draws some conclusions about what can be expected from satellite data sets as regards to the control of the oceanic mixed layer.

## 2. Two Interannual Simulations

[8] The OPA OGCM used is based on primitive equations [*Madec et al.*, 1998]. The present version, called ORCA, is a free surface version [*Roullet and Madec*, 2000] similar to the version used in D02. The vertical eddy coefficients are computed from a 1.5 turbulent closure model in which the evolution of the turbulent kinetic energy is given by a prognostic equation [*Blanke and Delecluse*, 1993]. The model domain is global. It has a 2° zonal resolution and a meridional resolution varying from 0.5° at the equator to 2° poleward of 20° latitude. The model has 31 vertical levels, and the vertical resolution varies from 10 m in the first 120 m to 500 m at the bottom. The model has been validated against in situ observations in the tropical Pacific and used extensively for process studies. For example, *Vialard et al.* [2001] and *Vialard et al.* [2002] used it to shed light on the ocean processes driving SST and SSS during the 1997–1998 ENSO event.

[9] In order to get an insight into the sensitivity of the model's mixed layer structure to the forcing fields applied, we performed two simulations covering the same period (1993–1998), using two different atmospheric state-of-the-art products: Simulation 1 (SIM1) uses forcing fields derived from the NCEP reanalysis [*Kalnay et al.*, 1996]. In simulation 2 (SIM2) the wind stress field is a combination of ERS 1–2 scatterometer-derived and TAO-derived wind stresses [*Menkes et al.*, 1998]. The precipitation field comes from *Xie and Arkin* [1996]. All other fluxes (evaporation and heat fluxes) come from the ECMWF reanalysis [*Gibson et al.*, 1997].

[10] Prior to these interannual simulations, the model was spun up during 6 years, which ensured a dynamic adjustment of the upper ocean in the tropics. In both simulations, SST was weakly relaxed toward *Reynolds and Smith* [1994] weekly field, using a relaxation coefficient of $-40\text{W m}^{-2}\text{ K}^{-1}$. This was meant to avoid dramatic drifts of the model SST field. However, this value of the relaxation coefficient does not constrain the model variability more than is acceptable, as we will see later in the differences between the two simulations. Regarding the model surface salinity field, it was left free in both simulations.

[11] An exhaustive validation of each run is clearly beyond the scope of the present study. Both simulations reproduce the large-scale features of the tropical Pacific ocean, in terms of currents, temperature and salinity, and the simulated patterns are consistent with previous studies [e.g., *Vialard et al.*, 2001]. As an example, we present the time evolution of the SSS along the equator (Figure 1). Both runs exhibit a well-marked salinity front separating the low surface salinity waters of the so-called Warm/Fresh Pool in the western part of the Pacific Ocean from the saltier water of the central basin. The front migrates at interannual timescales, in relation with ENSO variability. This is consistent with both observations and numerical studies (for further details, see *Vialard et al.* [2002, Figure 6b]). Both runs also reproduce the observed seasonal SSS cycle in the eastern part of the basin, although modulated by the ENSO signal, with minimum SSS during boreal spring at times of minimum equatorial upwelling. In the same way, both simulations are consistent with the previous numerical and observational studies as regards to SST, both in terms of large-scale mean structure and dominant variability patterns (not shown).

[12] Despite a qualitatively good overall agreement of both simulations, there are significant discrepancies in the simulated upper thermohaline structure. As an example, the time evolution of SSS along the equator for the 1997–1998 El Niño is relatively different between SIM1 and SIM2: the haline front in SIM1 remains strong throughout the period, whereas it virtually disappears in SIM2 during the first half of 1998 (Figure 1b). Computation of the root mean square (RMS) of the differences between SIM1 and SIM2 gives 0.6 psu in terms of SSS on average over the tropical Pacific basin. Most of these differences correspond to a bias in salt as seen on the difference of mean salinity between the two simulations (Figure 2a). In an area spanning most of the western equatorial basin and over a region slightly north of the South Pacific Convergence Zone (SPCZ), the long-term mean SSS is too salty by more than 1 psu in SIM2 as compared to SIM1. Those differences are partly related to the differences in evaporation-precipitation (E-P) forcing fields used for the two simulations (Figure 2b). In terms of SST, the differences between SIM1 and SIM2 are also marked, and the RMS difference of SST amounts to 1.0°C (not shown here). The biases in temperature and salinity throughout the mixed layer result in significant differences in the contribution of the mixed layer to the 0/60 dbar dynamic height anomalies (Figure 2c). Over most of the south-central tropical Pacific basin, the bias exceeds 5 dyn cm, which is of same order as the RMS amplitude of sea level variability. Auxiliary calculations, at basin scale, showed that both temperature and salinity are almost equally responsible of the bias in dynamic height. Locally, a 1 psu difference in salinity throughout the 0/60 m depth accounts for the 6 dyn cm difference in the 0/60 dbar dynamic height anomalies.

[13] It seems difficult to determine which simulation, SIM1 or SIM2, is the most realistic. With regard to the mean SSS field, the differences between SIM1 and SIM2 are of the same order as the differences between one simulation and climatological SSS from either *Levitus et al.* [1994] or *Vialard et al.* [2000] (not shown), with spatial patterns of those long-term SSS differences depending on the climatology used. Those comparisons must be considered with care since both observed SSS climatologies were not computed over the same period as the simulations. A more rigorous assessment of the simulated SSS field was made, based upon an exhaustive comparison with in situ SSS measurements from the TSG (ThermoSalinoGraph) network spanning our period of interest [*Hénin and Grelet*, 1996]. Some of these measurements, made along ship tracks, sample the western tropical Pacific basin relatively well. Figure 3 shows the differences in SSS along the so-called "Western Track", both in terms of mean and variability. Even though there is a good qualitative consistency between the three data sets, with lowest SSS under the Inter Tropical Convergence Zone (ITCZ) and SPCZ, and maximal variability in the equatorial region, there are marked

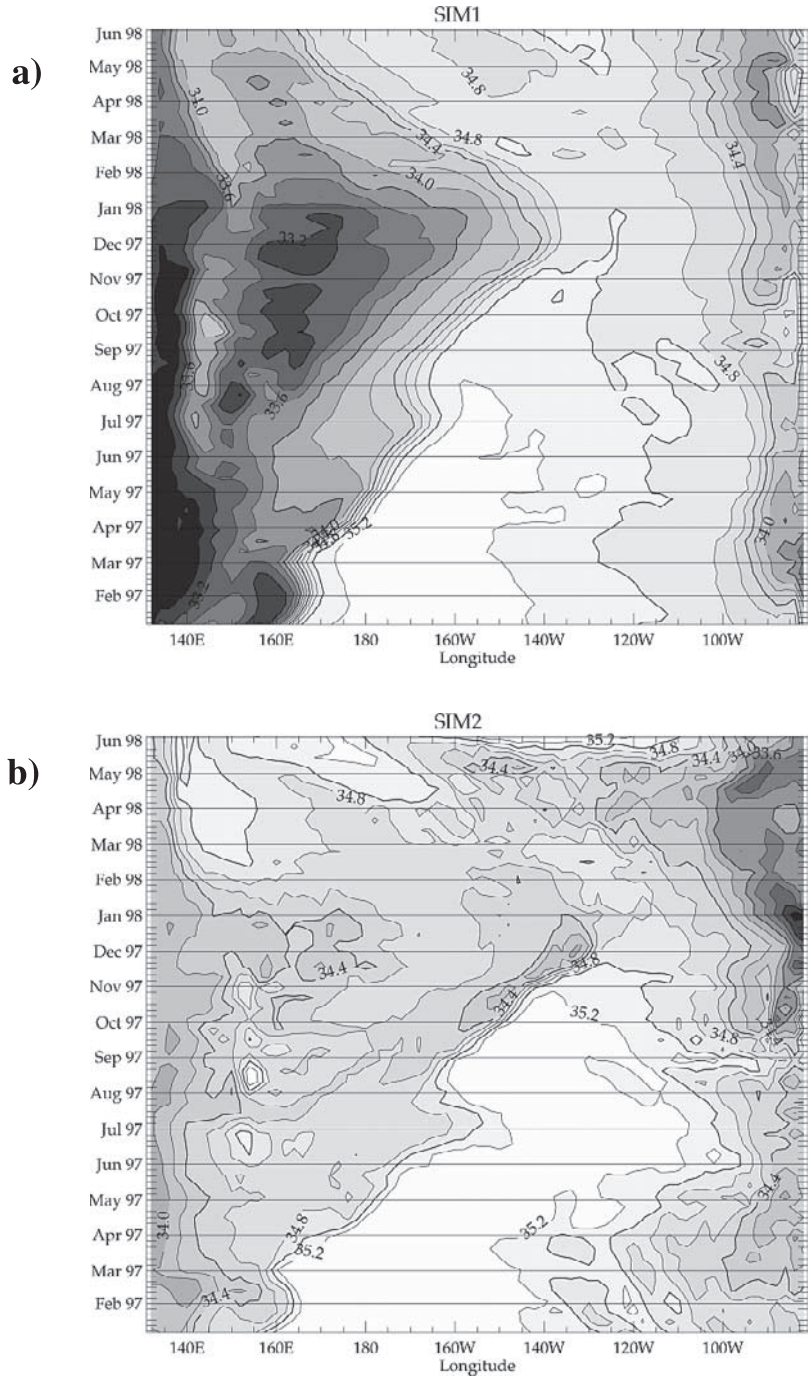


**Figure 1.** Longitude-time plot of SSS along the equator for (a) SIM1 and (b) SIM2. Iso-contours are every 0.2 psu.

discrepancies in the mean structure and in the variability patterns. On the whole, these analyses lead to the conclusion that both simulations present similarly high levels of overall error, both in terms of bias and variability.

[14] At this stage, one can conclude that the differences between SIM1 and SIM2 in both temperature and salinity are quite representative of the order of magnitude of the differences that currently exist between any state-of-the-art simulation and (poorly known) reality. These two simulations will therefore be considered as relevant for investigating the issue of bias and variability correction by data assimilation. Our conclusions from twin experiments should also have some relevance to any real data assimilation experiment, when these data become available.

## 3. Assimilation Experiments

### 3.1. Experimental Strategy

[15] As in D02, this study is based on classical OSSEs. We chose arbitrarily one of the two simulations presented in section 2 as our reference (REF in the following), from which we extracted the simulated observations to be

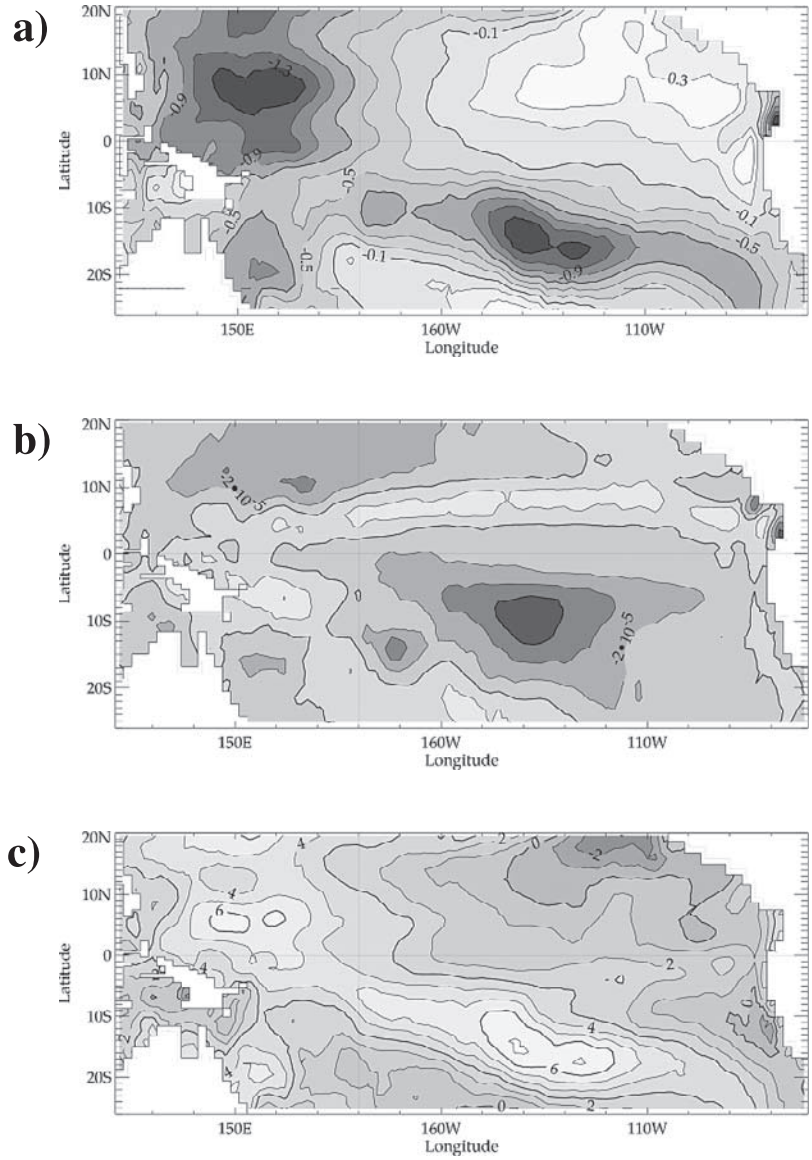


**Figure 2.** (a) Time-averaged difference in SSS between SIM1 and SIM2 over the 1997–1998 ENSO event. Iso-contours are every 0.2 psu. (b) Time-averaged difference in evaporation-precipitation forcing flux applied between SIM1 and SIM2. Iso-contours are every $2.10^{-5}$ kg $m^{-2}$ $s^{-1}$. The period of computation spans 1993–1998. (c) Time-averaged difference in 0–60 dbar dynamic height anomaly. Iso-contours are every 1 dyn cm. The period of computation spans January 1997 to June 1998.

assimilated. The model with and without assimilation (ASSIM and FREE, respectively) was forced with the other data set presented. Thus REF and ASSIM versus FREE will make it possible to evaluate the performance of assimilation: ASSIM is expected to generate a trajectory that is closer to REF than FREE. Assimilation results can be sensitive to the choice of REF: indeed at a given point, according to the choice of REF, the assimilation will have a stabilizing (destabilizing) effect on the water column if it produces a negative (positive) density increment in the mixed layer, which can result in a fairly different behavior of the assimilating model. In order to test the robustness of assimilation results, we performed sensitivity tests, choosing successively SIM1 and SIM2 as the reference run. This did not lead to any significant difference of assimilation performance therefore proving that our results are not dependent on the arbitrary choice of REF. In the following paragraphs, we present only the first set of experiments where SIM1 is used as REF and SIM2 as FREE.

[16] The simulated data considered in the subsequent experiments, and assumed to represent ocean surface satellite data, include the following.

[17] 1. SSS data, which are sampled according to the proposed *Global Ocean Data Assimilation Experiment* [*GODAE International Project Office*, 2000] accuracy requirement for large-scale studies ($2° \times 2° \times 9$ days resolution, noise level of 0.2 psu).

[18] 2. SST data, which are defined according to the current global observed fields available ($0.5° \times 0.5° \times 9$ days resolution, noise level of 0.5°C) [*Reynolds and Smith*, 1994].

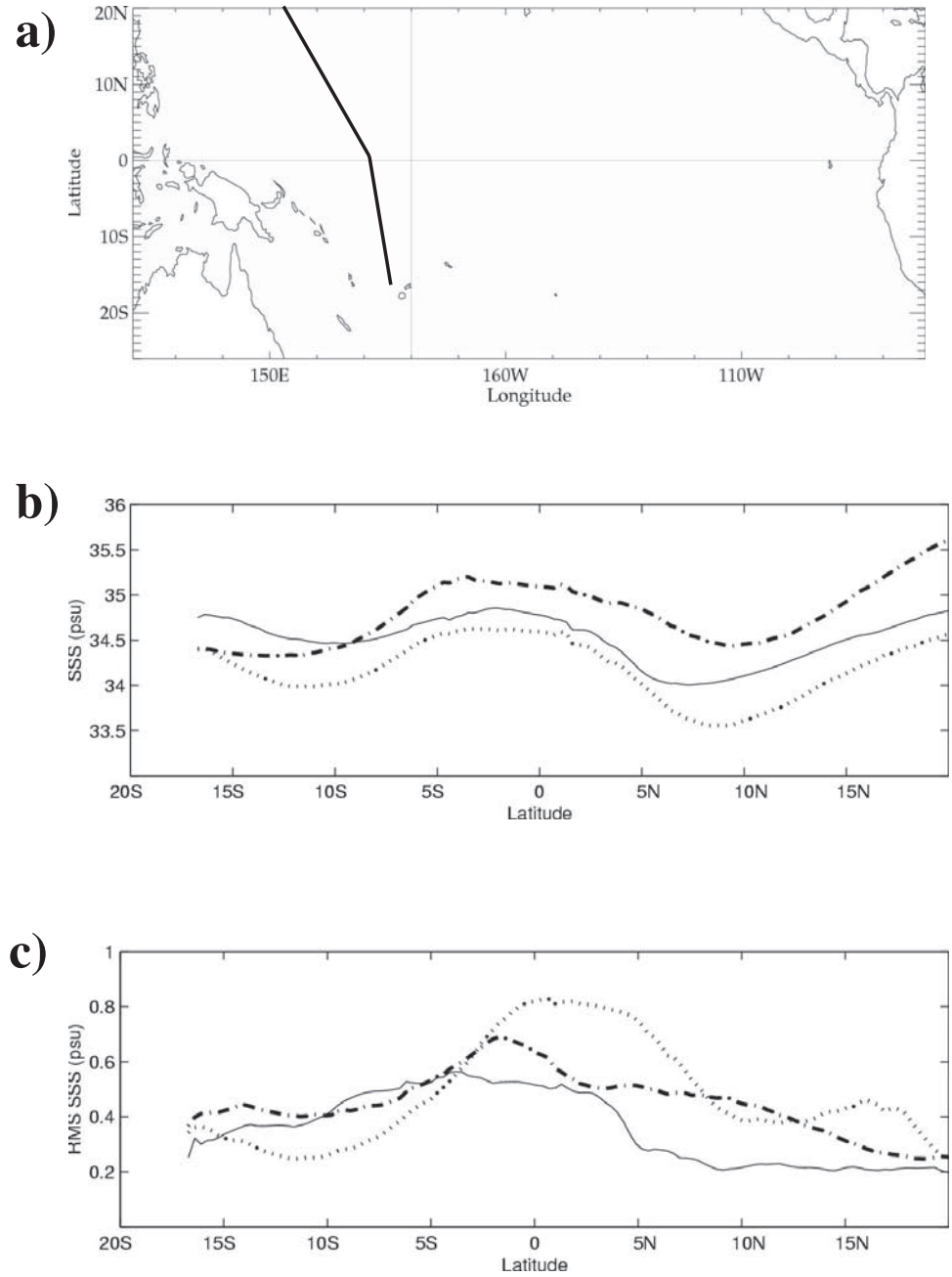


**Figure 3.** Comparisons between observed and modeled SSS. (a) Ship track along which SSS data are sampled. (b) Mean and (c) RMS of SSS along the track for the observations (continuous line), SIM1 (dotted line) and SIM2 (dash-dotted line). The period of computation spans 1993–1998.

[19] 3. SZC (Surface Zonal Current) data, whose use has been motivated by the availability of surface current data from *Bonjean and Lagerloef* [2002] ($1° \times 1° \times$ 9days resolution, background noise level of 8 cm $s^{-1}$ increasing to 24 cm $s^{-1}$ at the equator). For the sake of simplicity, they are defined onto the model grid. The reason for using such data is explained in section 4.2.1. Note that in real experiments, some correlations could exist between model and observation errors because the wind product goes into both the model and the ''observations''.

[20] All simulated data products are gridded. In a real-life context, the gridding procedure should lead to observational error covariance patterns at short scale. For example, the error spatial scale of satellite-derived SST data is typically of several hundreds of kilometers [*Reynolds and Smith*, 1994]. What is important in an assimilation scheme is the coherency between the errors and their statistical definition. For the sake of simplicity, the errors are supposed to be uncorrelated throughout the present paper, and defined by a diagonal observation error covariance matrix. Data are noisy by their respective error, and are assimilated every 9 days.

[21] First, to assess the assimilation performance, and the assimilation system, we performed a short time assimilation experiment. A three month period was found long enough. The period of interest spans the first 3 months of 1997, i.e., the period prior to, and including, the onset of the 1997–

1998 ENSO event. Second, we carried out a longer time experiment covering the whole 1997–1998 ENSO event, from January 1997 to June 1998. The assimilation experiments start on 1 January 1997, with FREE initial conditions. Assimilation schemes of increasing complexity order were used, starting with the standard version of the SEEK filter, to end with an adaptive version of the SEEK filter. These methods are presented with some details below.

### 3.2. Assimilation Methods

[22] The assimilation scheme is based on the SEEK filter, as in D02. The reader is referred to this paper for details about the inner structure of the SEEK algorithm. The basic assumption of the SEEK filter consists of specifying a forecast error covariance matrix ($P^0$) of reduced rank. The model error covariance matrix is simply defined as a fraction of the forecast error covariance matrix (see *Pham et al.* [1998] for further details). In our case, $P^0$ is represented by a limited number of three-dimensional multivariate EOFs (MEOFs), accounting for the dominant modes of the FREE model surface variability in salinity, temperature and zonal current. Typically, we use 10 modes computed over the 1993–1998 period that are enough to explain over 90% of the variance of SSS and SST. The 3-D multivariate approach allows information from the surface-only observed quantities to be spread to the whole state vector through the Kalman filter algorithm.

[23] The assimilation scheme was modified in the course of this study. Indeed, the conclusions of the first experiment presented in section 4 led us to apply the idea of an ''apprentice filter'' [*Brasseur et al.*, 1999]. It resulted in a modified version of the SEEK filter based on the concept of ''statistical learning''. Basically, it consists of sequentially enriching the error subspace of the SEEK filter using the residual information left in the innovation vector after each analysis step. In practice, at each assimilation stage, the mode, among the initial 10 modes composing the reduced basis, which is the most orthogonal to the innovation vector (defined by the differences between the forecast state and the data assimilated) is located. This least relevant mode is discarded, and we reconstruct a new mode based on the part of the innovation vector which is not projecting onto the initial error basis. Obviously, this new mode is rigorously defined within the observation space. The extrapolation of the ''apprentice'' mode from the surface observation grid to the surface model grid is done by a simple bilinear interpolation which is relevant in that case where observations have a coverage similar to the model grid. More care is required for the downward extrapolation from the surface model grid to the whole 3D state vector grid. Here we invoke physical considerations within the assimilation scheme: error is assumed to be strongly correlated, from the surface down to the depth of the mixed layer (isothermal layer) for salinity (temperature). The reader is referred to *Sprintall and Tomczak* [1992] for the definition of these depth criteria. Hence we extrapolate the ''apprentice'' SSS (SST) mode from the surface down to the forecasted depth of the top of the pycnocline (thermocline) for salinity (temperature), using a priori vertical covariances computed from the FREE run at every grid point. Typically, these covariances correspond to a correlation coefficient ranging from 1 at the surface to 0.7 at the maximal extrapolation depth. They were found consistent with previous studies [e.g., *Vialard and Delecluse*, 1998] and independent of the simulation considered.

[24] At this stage, we have built a new 3D bivariate (SSS, SST) error mode. It contains not only the physical information relevant to constrain the model trajectory but also the observation noise. Unfortunately, we are in an unfavorable case since the signal-to-noise ratio of the observations is of order of one, both in temperature and salinity. Hence the new error mode is strongly noisy, and it may not be consistent with the model equations, introducing spurious analysis. To filter out the noise and to balance the new mode patterns with the model equations, we used an ad hoc version of the model to run with this new mode. The horizontal diffusivity of the model was increased in the temperature and salinity equations (a viscosity coefficient of $10^4$ $cm^2/s^2$ was chosen) in order to smooth out the observation noise. It results in a weak perturbation of the model dynamical behavior (C. Maes, personal communication, 2002). Seven days of evolution of the new mode by this model seems to be a good compromise to balance it with the model equations by filtering out a great part of the noise without dissipating too much the physical signal of interest. After this procedure, we obtained a new, low-noise error mode, dynamically balanced, ready to be incorporated in the reduced basis of the SEEK filter to perform the data assimilation.

[25] This adaptive procedure is illustrated in Figure 4. It presents the ''apprentice'' mode, calculated at the first assimilation stage, before (Figures 4a and 4b) and after (Figures 4c and 4d) the time evolution by the diffusive version of the model. We can see clearly how the horizontal mode is projected downward, and how it is filtered by the model evolution. This plot illustrates also a possible drawback of this adaptive process. As an example, at 15°S–170°W the salinity increment originally limited to the upper 40 m (Figure 4b) extends down to 60 m depth once it has evolved in time (Figure 4d). In regions where the error mode exhibits positive salinity and/or negative temperature increments at the surface, the resulting positive density increment at the surface could destabilize the water column, and penetrate too deep when the model evolves. The risk is to impair the stratification in the upper part of the pycnocline (around 50 m) when the analysis is performed. This potential limitation of the assimilation scheme is investigated in further detail in section 5.

## 4. Statistical Assessment of the Assimilation Experiments

[26] The assimilation experiments were statistically assessed by computing the RMS differences (RMSD) between the ASSIM and REF runs, normalized by the corresponding RMSD between FREE and REF. Assimilation will have a positive (negative) impact if the ratio RMSD(ASSIM-REF)/RMSD(FREE-REF) is less than (greater than) 100%. We selected three depths: the surface level (where the assimilated data are defined), a level characteristic of the bottom of the mixed layer (60 m) and a level located at the mean thermocline depth (100 m). When SSS and SST only are assimilated together, the experiments are named SS-ST; when SSS, SST, and zonal surface velocity are assimilated all together, the experiments

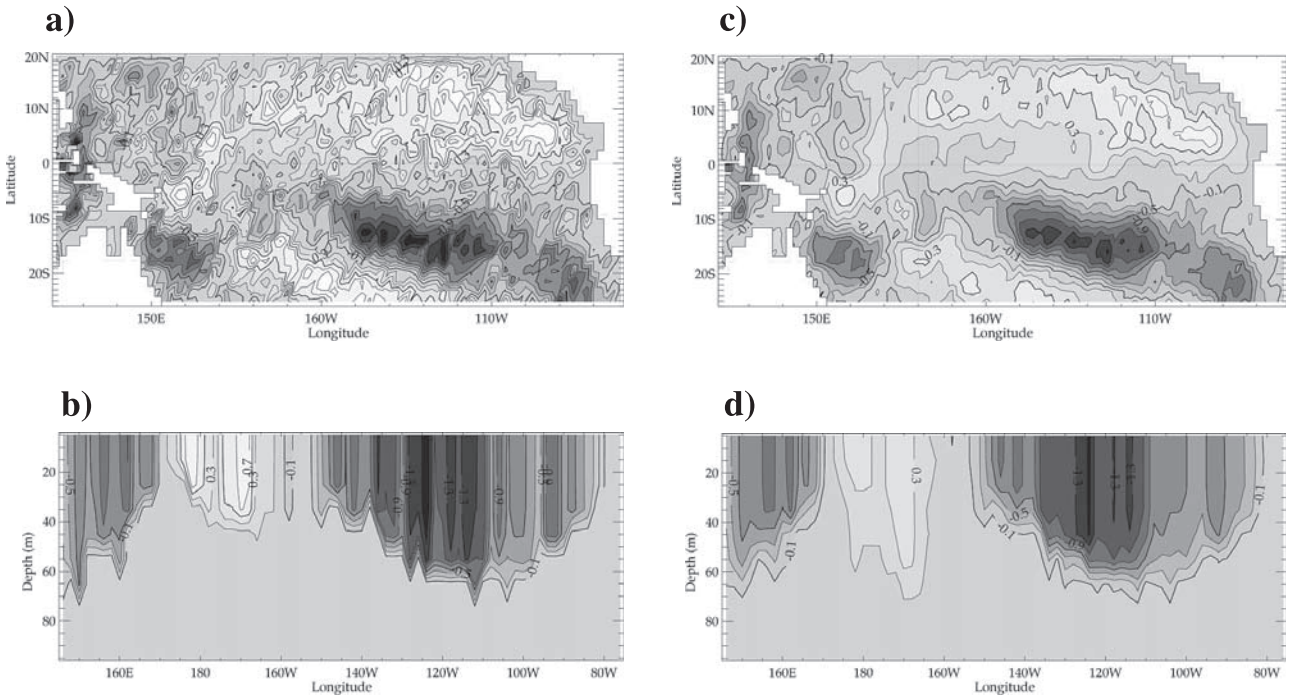


**Figure 4.** Salinity adaptive error mode diagnosed from SSS data on 1 January 1997: (a) surface structure prior to the evolution of the mode, (b) corresponding longitude-depth section along 15°S, and (c) and (d) same as Figures 4a and 4b after a 7 days evolution by the diffusive version of the model. Isocontours are every 0.2 psu. Darkest for lowest values.

are named SS-STU. The standard SEEK filter was first used (section 4.1), and results from the adaptive SEEK are presented in section 4.2

### 4.1. Standard SEEK Filter

[27] The SS-ST experiment is intended to determine how the conclusions gained in the favorable context of D02 apply to the present experimental conditions, where the consistency between error statistics of the SEEK filter and the innovation sequence of the assimilation is no longer assumed. Notably, the reduced basis, computed from a MEOF analysis of FREE, may incompletely account for the differences between REF and FREE simulations (see section 2). Results are presented for salinity only (Figure 5), as the conclusions also apply to the rest of the state vector. After the first assimilation time stage, salinity RMS error was reduced to a residual level of 75% at the surface and 85% at 60 m depth. It corresponds to a 45% and 30% error variance reduction, respectively. The corresponding residual errors in physical quantities were 0.45 (resp. 0.30) psu RMS at the surface (resp. 60 m). At 100 m depth, the effect of assimilation was hardly noticeable in terms of RMSD, with residual errors of about 0.4 psu RMS. Afterward, the error remained stable over time around this residual level whatever the chosen depth.

[28] These results are rather disappointing, as compared to the performance of the SEEK filter in the idealized experimental context of D02, where the assimilation of satellite-type SSS data led to residual errors in SSS smaller than 0.07 psu rms. Unlike this earlier study, assimilation was unable to converge to an acceptable level. If there is no real degradation of ASSIM as compared to FREE, the ASSIM solution remains far from REF. For instance, the large-scale contrast in SSS between the fresh pool of the West and the saltier water of the central equatorial basin (Figure 1) is poorly controlled by assimilation (not shown). The relatively poor performance of the standard SEEK filter was foreseeable to a certain extent. Indeed, it can be explained by two main reasons. First, at initial assimilation stage a significant part of the innovation vector, which is characteristic of a bias, and different variability modes between REF and FREE (see section 2) cannot be explained by the MEOFs error modes used by the SEEK filter. For example, 55% of the initial innovation variance in SSS and SST is orthogonal to the original error modes. Then, with time, it appears that the SEEK filter does not manage to further improve the control of the model trajectory. This can be explained by a crude model error defined as a fraction of the forecast error covariance matrix (see section 3.2). It means that no new directions are defined in order to update the error covariance according to the actual errors generated by the forcing fluxes in the course of the model run. The difficulty to define a realistic model error is one reason for the use of an adaptive assimilation scheme. At this stage, one can conclude that, within a realistic experimental context, assimilation of SSS and SST satellite-type data with the standard SEEK filter does not allow proper control of the mixed layer thermohaline structure.

### 4.2. Adaptive SEEK

#### 4.2.1. SS-ST Assimilation: The Equatorial Problem

[29] In the light of these results, we then modified the assimilation scheme to use an adaptive SEEK filter as described in section 3.2 and performed an assimilation experiment similar to the one in section 4.1. The results are presented on Figure 6. One can see the positive impact of the new assimilation scheme in temperature and salinity through-

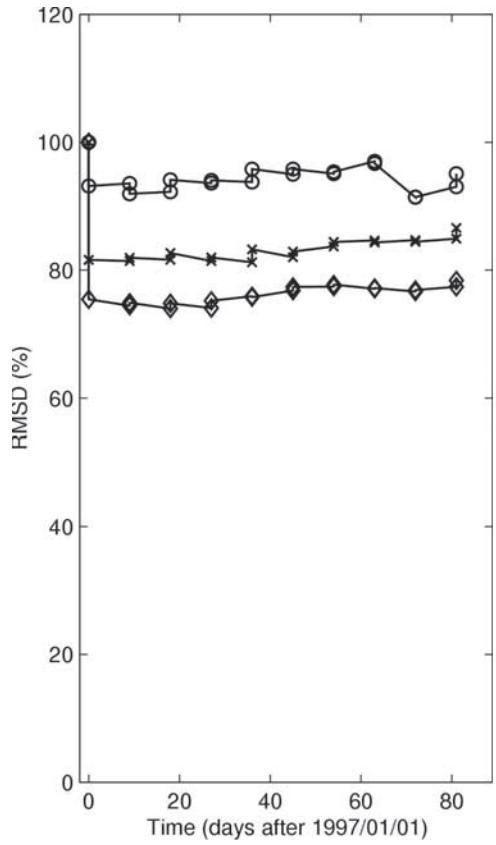


**Figure 5.** Impact of assimilation of SSS and SST with standard SEEK filter on salinity field. Three depths are selected: the surface (diamonds), the mean mixed layer depth (60 m, crosses), and the thermocline (100 m, circles). The time evolution of the error RMSD (SIM1-ASSIM) is defined as a percentage of the error RMSD (SIM1-SIM2). Both the prediction and the analysis stages are plotted. Statistics are computed over the whole tropical Pacific Ocean (120°E–90°W; 20°N–25°S).

out the upper ocean. At the surface, the residual error decreases to 35% and 30%, respectively for SSS and SST. It corresponds to residual errors of 0.17 psu RMS and 0.40°C RMS respectively which are less than the corresponding observation noise level. The assimilation method is also effective for propagating the surface information downward, with a 60% reduction of error at 60 m depth (0.3 psu, 0.8°C residual RMS errors), a positive impact of assimilation down to 100 m, and no visible degradation below. Over time, errors remain relatively stable. Generally, the SS-ST assimilation seems to perform relatively well.

[30] Despite the successful results, a noticeable degradation occurs in the equatorial region. It is linked to the poor control of zonal current in the mixed layer at the equator. This problem has already been noted in other assimilation systems [*Bell et al.*, 2001; *Burgers et al.*, 2002; *Weaver et al.*, 2002]. It is related to the peculiar physics of the equatorial oceans. Along the equator, the zonal current at the surface results from a balance between the influence of the trade winds that tend to accelerate it westward and the zonal pressure gradient that tends to accelerate it eastward. With regard to this experiment, during the first two months of 1997 in the central equatorial Pacific, the NCEP trade winds in REF were weak, in equilibrium with a weak zonal pressure gradient, which resulted in a South Equatorial Current (SEC) velocity of less than $-40$ cm.s$^{-1}$; on the other hand, the FREE simulation is forced with stronger ERS+TAO trade winds, which are in equilibrium with a stronger zonal pressure gradient in the upper ocean, resulting in a faster SEC (reaching $-60$ cm s$^{-1}$). In terms of upper ocean temperature and salinity, ASSIM presents a weak zonal pressure gradient in accordance with REF but not in equilibrium with the model forcing. It means that an imbalance appears among the forces driving the SEC, and it accelerates constantly over time with a peak value greater than 160 cm s$^{-1}$, rendering the advection of temperature and salinity totally unrealistic. The mean difference in terms of surface zonal current between ASSIM and REF exhibits strong errors in the SEC, superior to 40 cm s$^{-1}$ over most of the central equatorial basin (Figure 6c).

[31] In conclusion, the results of this experiment appear satisfactory except in the equatorial band. At this stage, various avenues can be investigated to solve the problem. A possible solution would be to use the correlation that exists in the equatorial Pacific between SST and zonal wind stress [*Picaut et al.*, 1997] so as to infer wind stress correction from SST correction. This would be somewhat equivalent to making use of a coupled ocean-atmosphere model, which is clearly out of the scope of the present study. Here, the work focuses on assimilation of surface-only oceanic data. Consequently, we decided to take advantage of the knowledge of surface (geostrophic and Ekman) current data estimated from altimetry and wind stress [*Bonjean and Lagerloef*, 2002] by assimilating them in addition to SST and SSS data to better constrain the modeled surface current, particularly in the equatorial band. This is presented in the following section 4.2.2.

#### 4.2.2. SS-STU Assimilation

[32] Using mainly satellite sea level anomaly and wind stress data, *Bonjean and Lagerloef* [2002] derived gridded ocean surface currents with a satisfactory degree of accuracy for the monitoring of the large-scale circulation. Typical errors are of 8 cm s$^{-1}$, except in the equatorial band where errors can reach 24 cm s$^{-1}$. This quality appears satisfactory as regards to the error of O(1m s$^{-1}$) generated in the previous experiment. The same adaptive procedure as described in section 3.1 for SST and SSS data was used for current data and it resulted in a trivariate temperature-salinity-zonal current ''apprentice'' error mode calculated at each assimilation stage. Therefore we extended the adaptive SEEK filter to the assimilation of SSS + SST + Surface Zonal Current data.

[33] We conducted the same experiment as in section 4.2.1. The results are presented on Figure 7. The impact of this assimilation on the surface zonal current is clearly visible (compare Figure 7c and Figure 6c). The high error in the equatorial band has been reduced by a factor of 2 (30 cm s$^{-1}$ versus 60 cm s$^{-1}$). Averaged over the basin, the RMS error level is about 17 cm s$^{-1}$, consistent with the observation error level of the current data assimilated. Below the surface layer, the residual error level is satisfactory with a 10 cm s$^{-1}$ error at 60 m and 100 m. Given this fairly good performance of the assimilation method in terms of zonal current, we can expect that the advection of

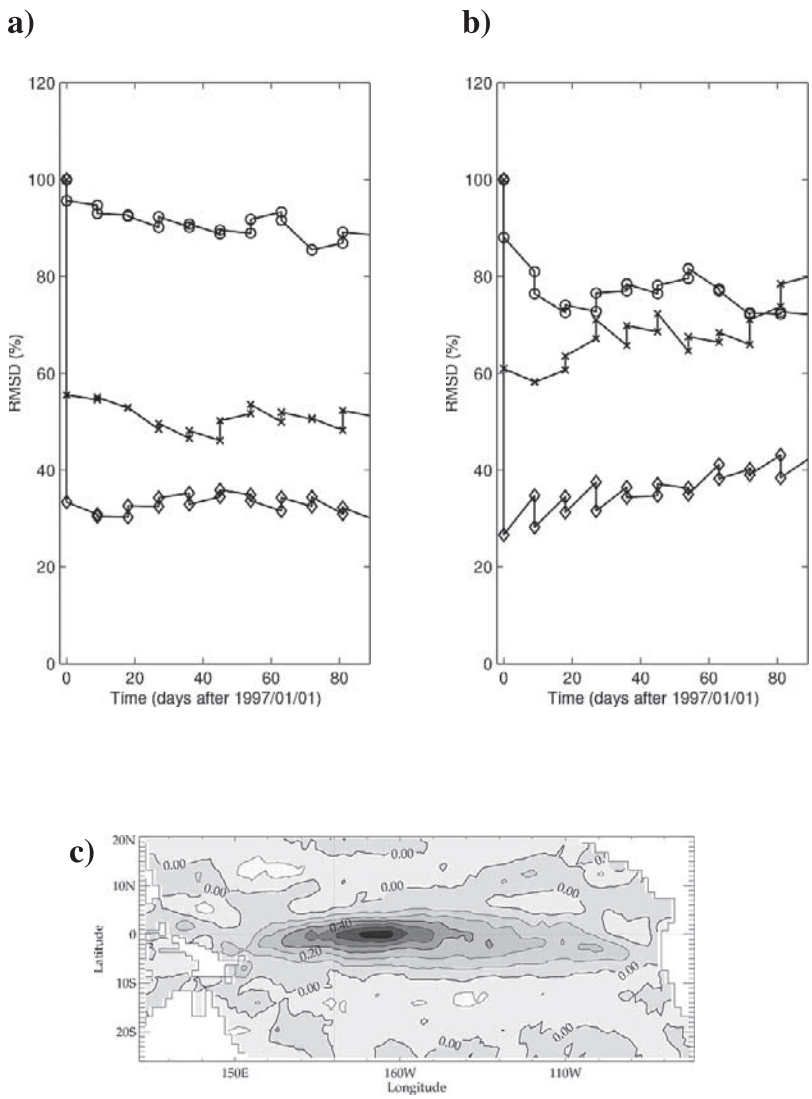


**Figure 6.** Same as Figure 5 but for the assimilation of SSS and SST with the adaptive SEEK filter, for (a) salinity and (b) temperature. The same three depths as in Figure 5 are selected. (c) Time-averaged difference in surface zonal current between REF and ASSIM fields. Iso-contours are every 0.1 m $s^{-1}$. The period of computation spans January to March 1997.

temperature and salinity in the equatorial band to be better reproduced. Hence, in terms of temperature and salinity only the assimilation performed slightly better than in the previous experiment, particularly at the surface.

[34] In conclusion, the adaptive version of the SEEK filter applied to the assimilation of satellite-type data of SSS, SST and surface zonal current seems relatively effective for the constraint of the upper thermohaline structure of the tropical Pacific. Therefore we investigated the results in more details with a longer assimilation experiment covering the whole 1997–1998 ENSO event. The outcome is presented in the next section.

## 5. A 1997–1998 Assimilation Experiment: The Mixed Layer Simulation

[35] So far, a short period of data assimilation (3 months) was considered long enough to draw initial conclusions about the worth of assimilation methods, and to decide on an adequate strategy for the assimilation and the choice of data to be used. In the following experiment, we investigated the results from a 1.5 year assimilation period, from January 1997 to June 1998, in order to assess assimilation performance. This period was chosen to cover strong El Niño/La Niña events, marked by a strong signature of the surface variables. We assimilated SSS, SST, and zonal velocity data (see section 4.2.2). Assimilation results were investigated in order to find out what information assimilation brought to the control of the oceanic mixed layer, characterized by its temperature and salinity homogeneity throughout its depth. In addition to temperature and salinity, the depth of the mixed layer is an important factor to be determined. It may be conditioned by the existence of a barrier layer in salt at the bottom of the density mixed layer. In real world, for the equatorial Pacific, the mixed layer depth varies in a range of 20–70 m, and the barrier layer thickness in a range of 0–40 m [*Delcroix et al.*, 1996; *Ando and McPhaden*, 1997]. These depths may be difficult to simulate

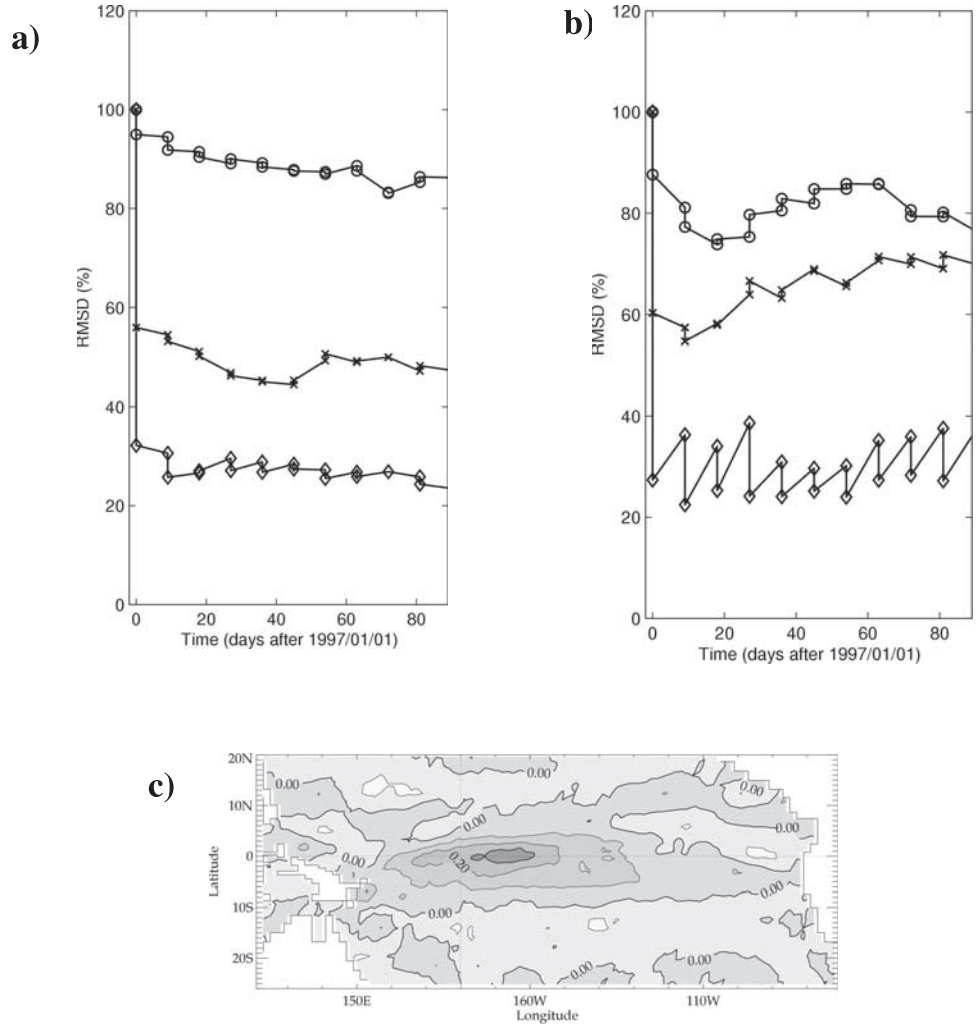


**Figure 7.** Same as Figure 6 but for the assimilation of SSS, SST, and surface zonal current with the adaptive SEEK.

accurately as the 10 meter vertical resolution of the model is rather crude. It is therefore a real challenge for the assimilation of surface-only data to have some positive impact on them.

### 5.1. General Analysis

[36] ASSIM results are first presented in accordance with the REF (SIM1) and FREE (SIM2) results shown in section 2, and covering the same 18 month period. By comparison with Figure 1a, the time evolution of SSS along the equator for ASSIM (Figure 8a) is satisfactorily reproduced even if the signal is a little noisy. The zonal salinity front of the eastern edge of the Fresh Pool is correctly simulated, both in terms of position and intensity. Notably, it becomes visible during the first half of 1998, unlike FREE (Figure 1b). The salty bias of the Fresh Pool surface waters is no longer perceptible. In the same way, the biases in SSS illustrated in Figure 2a at basin scale are well corrected in ASSIM (Figure 8b). A similar conclusion can be drawn with regard to the control of SST bias (not shown). As expected, the positive impact of assimilation is not limited to the observed part of the state vector. The 0–60 dbar mean dynamic height differences between ASSIM and REF are drastically reduced over most of the assimilation domain (Figure 8c), by comparison with Figure 2c, with differences less than 1 dyn cm in absolute values nearly everywhere. This means that both temperature and salinity are relatively well constrained in the model upper layers, and suggests the potential value of real surface data when they become fully available.

[37] Figure 9 presents the difference between the simulations with and without assimilation in term of mean density mixed layer depth and barrier layer thickness. The marked discrepancies between REF and FREE (Figures 9a and 9b) reveal the sensitivity of these quantities to the atmospheric forcing, something which has already been addressed in previous numerical studies [*Vialard and Delecluse*, 1998]. Errors are rather nonhomogeneous at basin scale, and the averaged RMS error is 18 m for the mixed layer depth, and 11 m for the barrier layer thickness. It is an interesting result to show that assimilation of surface-only data tends to have an overall positive effect on the estimation of these physical features (Figures 9c and 9d). Indeed, assimilation makes it possible to reduce the RMS error from 18 to 15 m for the mixed layer depth, and from 11 to 9 m for the barrier layer thickness. The effect is much better in the

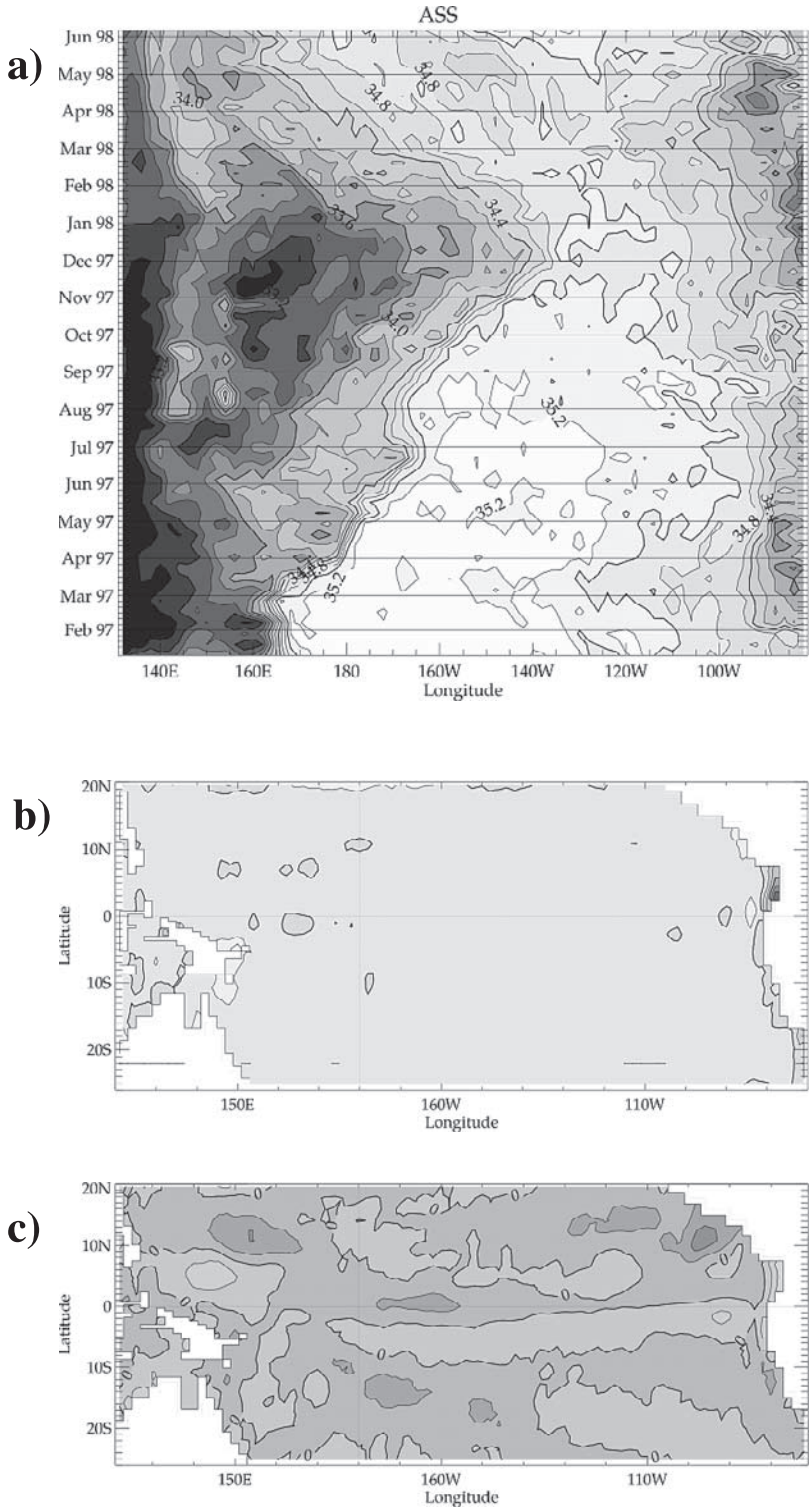


**Figure 8.** (a) Longitude-time plot of SSS along the equator for ASSIM. Time-averaged difference between REF and ASSIM over the 1997–1998 ENSO event in (b) SSS (iso-contours are every 0.2 psu) and (c) 0–60 dbar dynamic height anomaly (iso-contours are every 1 dyn cm).

western Pacific warm pool (say 10°N–10°S; west of the dateline), where the RMS error decreases from 19 m to 12 m for the mixed layer depth, in a region where the upper ocean vertical structure is important for ENSO mechanisms. This tends to validate the downward extrapolation of the surface data defined within the adaptive assimilation scheme previously described. Although the impact of assimilation is generally positive, assimilation does not perform as well everywhere, as for instance near 15°S–150°W, where ASSIM yields a mixed layer depth that is 25 m deeper than in REF. Several reasons can explain the regional difficulties of assimilation in simulating mixed layer depth and barrier

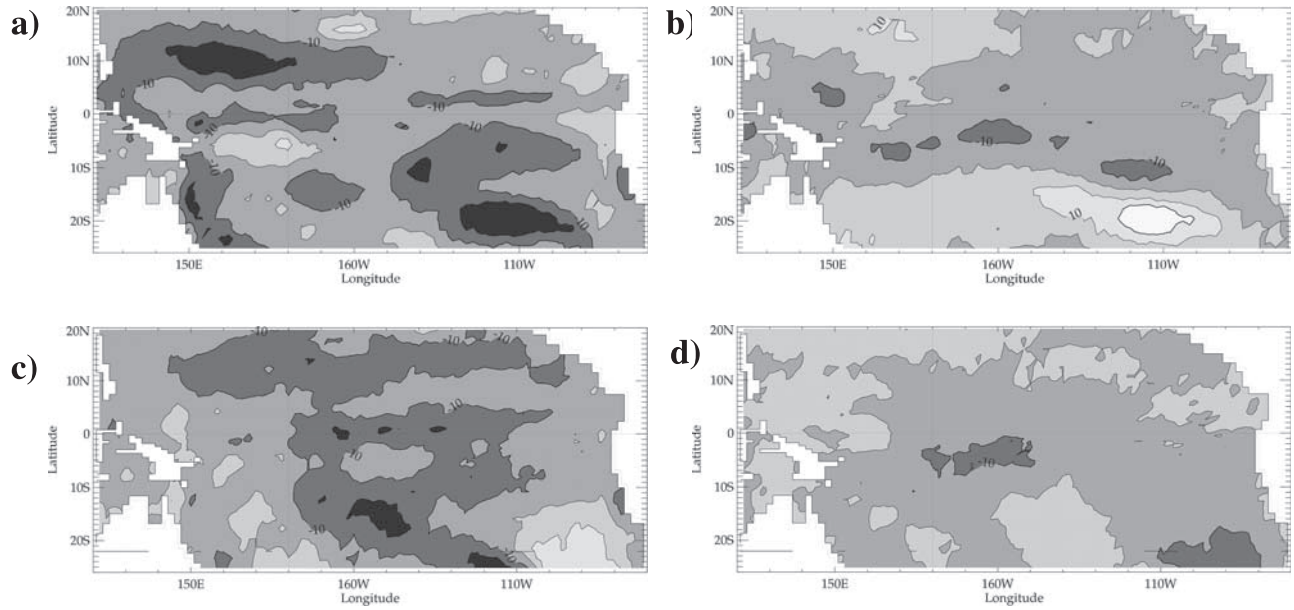


**Figure 9.** Time-averaged difference between REF (SIM1) and FREE (SIM2) for (a) the depth of the top of pycnocline, computed using *Sprintall and Tomczak*'s [1992] criterion, (b) the corresponding barrier layer thickness. (c) and (d) Same as Figures 9a and 9b but for the difference between REF and ASSIM. Iso-contours are every 10 m.

layer thickness. First, the pycnocline and thermocline depths estimated from the predicted state (ASSIM) and used to build the ''apprentice mode'' may be in error by comparison with REF. Second, the information introduced by the assimilation may destabilize the vertical equilibrium of the water column, and there is no control in subsurface to limit this possible degrading effect.

### 5.2. Local Analysis

[38] We wish to further illustrate the impact of the assimilation on the vertical structure. For this we chose three points, located in the ITCZ (8°N, 168°E), in the SPCZ (14°S, 170°W), and in the Warm Pool Areas (WPA, 0°N, 155°E) which exhibit strong variability signal in SSS. With regard to Figure 9, the ITCZ point seems positively impacted by ASSIM, and the SPCZ point negatively impacted by ASSIM. The WPA point is particularly interesting due to the special role of the mixed/barrier layer in the warm pool for ENSO events [*Delcroix and McPhaden*, 2002]. Mean and standard deviation of the vertical profiles in temperature and salinity are plotted in Figures 10, 11, and 12 for the SPCZ, the ITCZ, and the WPA points, respectively.

[39] At the SPCZ point, we can see strong differences between the REF and FREE profiles. At the surface, they are characterized by saltier (+0.5 psu) and colder (−1°C) water in FREE than in REF, and a salinity variability double in FREE compared to REF. Along the vertical, the stratification is more marked in REF than in FREE, with very different standard deviation salinity profiles. In FREE, the variability diminishes with depth, while in REF there is a peak in variability with depth (45 m depth) at the bottom of the mixed layer. Assimilation gives a good correction in the upper 30 m both in temperature and salinity. ASSIM presents mean vertical profiles more in accordance with REF, but not stratified enough. Thus the freshening and heating action at the surface extends too deep, which results in fresh and hot biases of the water column below 40–50 m compared to REF, leading to an erroneous estimation of the mixed layer depth. A positive impact of assimilation is clearly seen on the standard deviation salinity profile with an ASSIM variability which looks like the REF one, even if the maximum is too deep due to the incorrect estimation of the mixed layer depth. At this stage, ASSIM impacts positively on the simulation even if the downward influence of the assimilated surface data extends too deep due to the lack of vertical stratification in the FREE simulation.

[40] At the ITCZ point, the same general comments as above can be made on the mean REF and FREE profiles. FREE is characterized at the surface by a salty bias of 1 psu, and at 130 m by a hot bias of 3°C. Despite marked differences in both salinity and temperature between REF and FREE, ASSIM is successful in reproducing accurately the REF mean temperature and salinity profiles throughout the upper 200 m. This is rather impressive considering that the present assimilation configuration is designed to control the surface layers only. It can be explained by the possible role of the original reduced basis of the SEEK filter. In terms of standard deviation, REF exhibits stronger variability than FREE in the surface layers (the contrary is true for the SPCZ point), and ASSIM is relatively successful in correcting the variability in the upper 30–40 m. At depth, below the mixed layer, ASSIM exhibits too much variability, particularly in salinity. It shows the limitations of the present assimilation configuration.

[41] For the WPA point, by comparison with REF, the mean FREE salinity profile is characterized at the surface by a salty bias of the order of 1 psu and a vertical stratification that is too smooth. Despite these marked differences, ASSIM is successful in retrieving the ''true'' salinity profile throughout the upper 100 m. This is an interesting result,

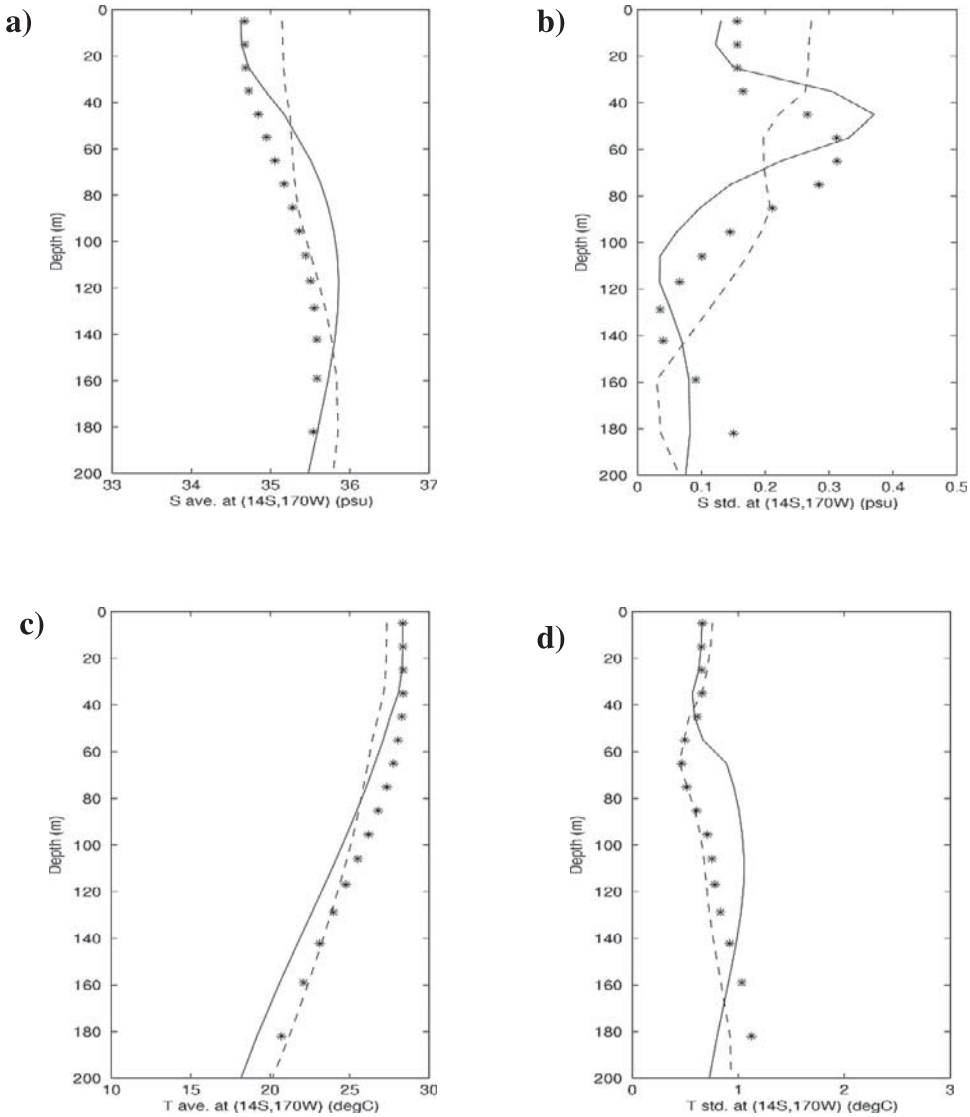


**Figure 10.** (a) Time-averaged salinity profile at (14°S, 170°W) for REF (continuous line), FREE (dashed line), and ASSIM (stars). (b) Corresponding profile of salinity standard deviation. (c) and (d) Same as Figures 10a and 10b but for temperature. Period of computation spans January 1997 to June 1998.

considering the role of salinity in the warm/fresh pool. For the mean temperature, there is little difference between REF and FREE at the surface, but the stratification is more pronounced in REF than in FREE. ASSIM is able to correctly simulate the mean thermocline. There is higher-salinity variability for REF than for FREE in the first 80 m depth. ASSIM brings out this high-variability level, even if the maximum of variability is 20 m too deep. For temperature, REF and ASSIM exhibit the same vertical variability structure, except that the maximum of variability is 40 m too deep for FREE compared with REF. ASSIM locates this maximum more accurately, but it performs poorly in reproducing its actual amplitude.

[42] We also investigated the time evolution of the specific fields characterizing the mixed layer (SSS, SST, mixed layer depth) and the barrier layer thickness at the WPA point (Figure 13). SSS FREE exhibits an almost constant strong bias during the entire assimilation period; as for SST, the differences are marked during the onset phase of El Niño (January 1997 to July 1997), and during the end of the La Niña assimilation period (March 1998 to June 1998). Consistent with the previous conclusions, assimilation controls both SSS and SST remarkably well. Concerning the mixed layer depth, FREE is characterized by a mixed layer extending too deep as compared to REF, and also by a higher variability, occurring at depths varying from 20 to 120 m. It is interesting to relate this local time evolution to the large-scale climatic context. The large oscillations in mixed layer thickness in March–April 1997 (Figure 13c) are related to the high-frequency westerly wind bursts that occurred over the western equatorial Pacific [e.g., *Lengaigne et al.*, 2002]. These wind events have been identified as potential triggers of 1997–1998 El Niño event [e.g., *McPhaden*, 1999]. The larger oscillations in FREE mixed layer thickness as compared to REF are likely to be due to more energetic wind bursts in ERS+TAO wind stress

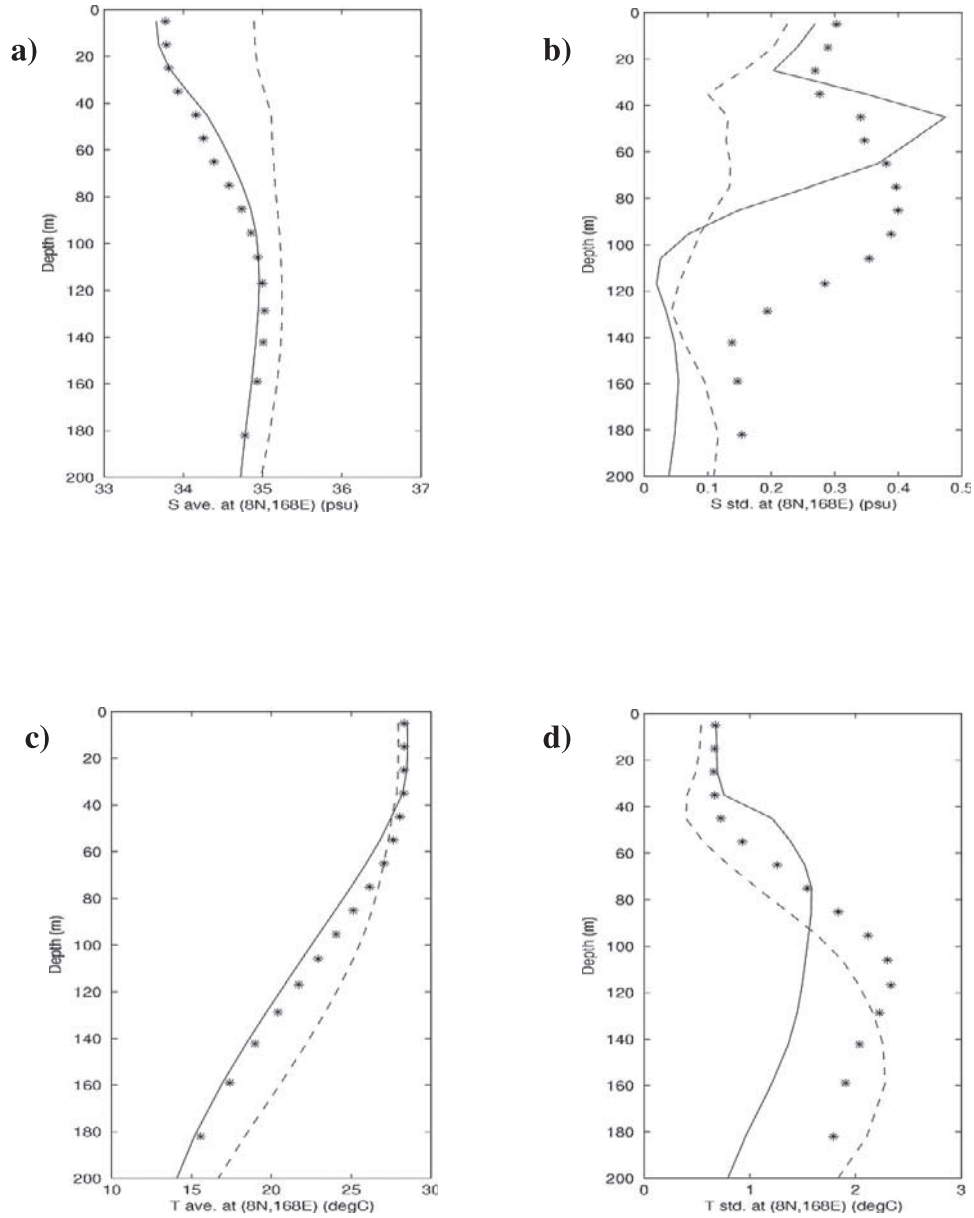


**Figure 11.** Same as Figure 10 at (8°N, 168°E).

[*Menkes et al.*, 1998] than in NCEP reanalysis [*Kalnay et al.*, 1996] (not shown). Assimilation partly allows to correct this overestimated variability, but the quality of the control is less impressive than for the surface variables. The mixed layer is more in phase with REF, becoming shallower in the first months of 1997 and during the period after March 1998. In terms of barrier layer thickness (Figure 13d), we observe a global decrease throughout 1997 for all simulations. This is consistent with the mechanism proposed by *Delcroix and McPhaden* [2002]: the barrier layer becoming shallow during this period, the entrainment of subsurface water from the main thermocline within the mixed layer becomes possible, which favors the cooling of surface water visible in Figure 13b. Performances of assimilation on the estimation of barrier layer thickness are less evident given the small amplitude (0–20 m) of this signal as compared to the vertical resolution of the model. A possible improvement can be seen in April–June 1997 when FREE simulates a barrier layer thickness of about 30 m while ASSIM (and REF) simulates a thickness of about 10 m. This last thickness agrees well with in situ observations [*Delcroix and McPhaden*, 2002] which showed that both the zonal salinity front located at the eastern edge of the warm pool and the area of thick barrier layer located a few degrees longitude to the west of this front moved east of the dateline at this time, resulting in an almost absent barrier layer at 0°–155°E. Overall, the impact of assimilation on barrier layer thickness seems qualitatively positive, a feature which may be crucial in prediction studies given the likely importance of the barrier layer for the onset of El Niño in the real world [*Lukas and Lindstrom*, 1991] and in coupled models [*Maes et al.*, 2002].

[43] At this stage, we have some idea of the behavior of our assimilation scheme for surface data. The adaptive

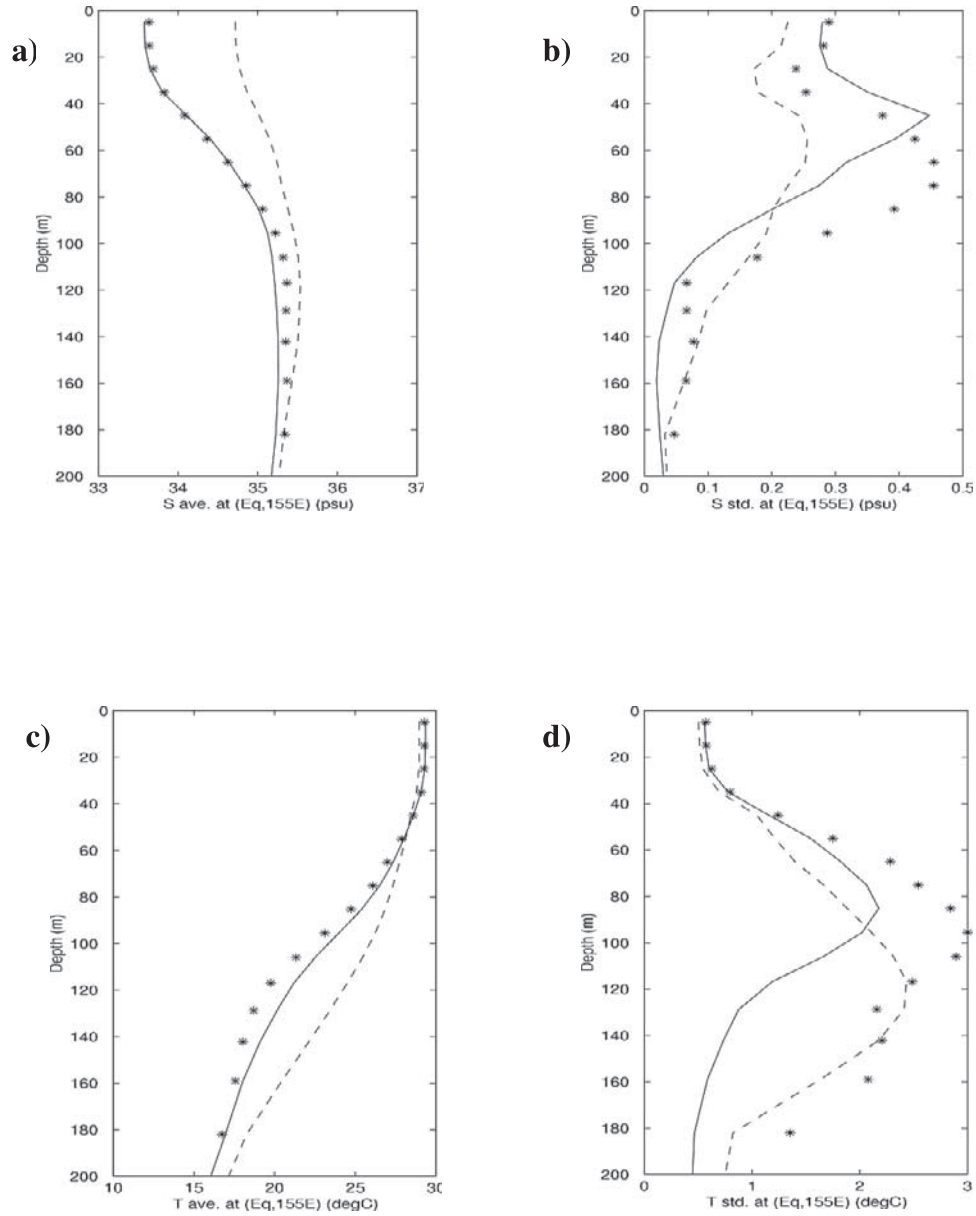


**Figure 12.** Same as Figure 10 at (0°N, 155°E).

SEEK filter, combining both the original reduced basis and an ''apprentice'' mode, seems relatively satisfactory in constraining the main mixed layer characteristics. It might also have some positive influence on the accuracy of the simulation of oceanic structure at greater depths, in terms of both mean and variability patterns. However, it is also clear that surface-only data are not sufficient to simulate realistically the subsurface dynamics of the ocean. The assimilation technique, while valuable, has some built-in limitations regarding downward propagation of surface information. Subsurface temperature and salinity data would usefully complement the surface observations.

## 6. Conclusion

[44] The objective of this work was to assess how surface-only satellite data such as SSS and SST could be used to improve the modeling of the mixed layer in the tropical Pacific Ocean, making use of an advanced data assimilation system. This study was motivated, on the one hand, by the recognition of the oceanic mixed layer as a key component of the climatic system, and, on the other hand, by the existence of ongoing and future satellite missions dedicated to measuring ocean surface parameters. In particular, SST and surface current (from altimetry, wind stress, and SST fields) are now routinely monitored, and SSS measurements are likely to become available within the next few years. From an assimilation viewpoint, these data sets are particularly interesting because they bring complementary information to the data currently assimilated. Typically, assimilation of altimetric sea level anomalies and in situ temperature profiles are relevant for the control of the subsurface layer, whereas SSS and SST data are intimately linked with the behavior of the mixed layer.

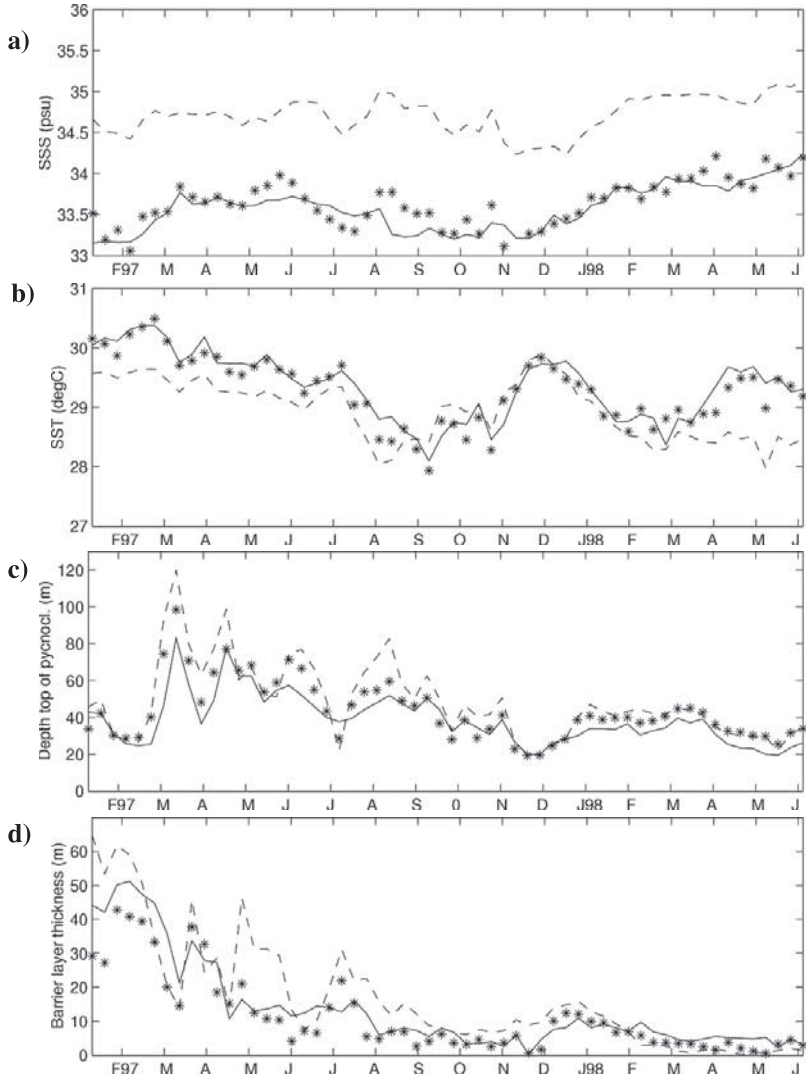


**Figure 13.** Time evolution of (a) SSS, (b) SST, (c) depth of top of pycnocline, and (d) barrier layer thickness at (0°N, 155°E) for REF (continuous line), FREE (dashed line), and ASSIM (stars).

[45] Since satellite SSS data are not available at this time, and to better analyze how assimilation works, we adopted an approach using twin experiments. The twin experiments were chosen with care to provide realistic conditions for assimilation. Notably, differences in terms of mean (bias) and variability between the model simulation and the assimilated synthetic observations were taken into account to be closer to assimilation experiments using real data. The simulations used for the experiments have errors in the range of the errors between any simulation and real observations. We implemented an adaptive version of the SEEK filter that allows to use much more efficiently the information contained in the assimilated data than the standard SEEK filter does.

[46] The assimilation of SSS and SST data gives fairly good control of the upper model layers, but a specific problem arises in the equatorial band. Inconsistencies between, on the one hand, the corrections brought by assimilation and, on the other hand, the atmospheric momentum forcing, are likely to impair drastically the quality of simulation there, particularly in terms of zonal velocity. This equatorial problem has already been evidenced recently by several authors. A solution could be to use a coupled ocean-atmosphere system; this is beyond the scope of the present study. To solve the problem we assimilated surface current data, deduced from altimetry and wind stress and routinely available, in addition to SSS and SST. In such a way, the assimilation scheme performs well with a significant error reduction at the surface, and extending to a depth of 100 m. The averaged residual errors are lower than the observational noise of the assimilated data: less than 0.17 psu, 0.3°C and 0.17 m $s^{-1}$ on SSS, SST and surface zonal current respectively.

[47] An assimilation experiment covering a period of a year and a half was then conducted, covering the 1997–1998 ENSO event characterized by strong interannual variability of the surface variables, and strong differences between the simulations used for the twin experiments. Initial errors on both temperature and salinity resulted in errors in the 0–60 dbar dynamic height anomalies reaching

6 dyn cm. We investigated the main characteristics of the mixed layer such as SSS, SST, mixed layer depth, barrier layer thickness. It appears that the control of the upper ocean (typically the 0–40 m layer) is efficient. Generally speaking, assimilation results in a better description of the vertical structure in the upper layers, which in turn results in an improved estimation of the mixed layer depth. Some slight improvement in terms of barrier layer thickness is also detectable, even if the limits of our assimilation scheme as well as the model vertical resolution are reached. Below the mixed layer, our results suffer from the lack of subsurface information needed to constrain the subsurface dynamics of the ocean, and to correct for potential errors in the depth estimation of the correction brought by the assimilation. Results are particularly noticeable in the convergence zones and, interestingly, in the warm pool region which is the key area for the ENSO phenomenon.

[48] To conclude, the adaptive SEEK filter was developed here for the assimilation of satellite-type surface data in order to be readily usable to assimilate real data as soon as they become available. Our assimilation scheme seems rather successful in its objective to control the main mixed layer characteristics. At greater depths, some additional information would be useful to better control the dynamics at the bottom of the mixed layer. From the point of view of satellite-derived data, assimilation of sea level anomalies may bring some useful constraint on the thermocline. It is also clear that subsurface in situ data, such as those derived from the TAO array and the new ARGO project, are essential to take advantage of the complementary nature of all these data sets. A joint assimilation of both satellite surface data and in situ subsurface data must be investigated.

[49] **Acknowledgments.** This work was partly supported by the Service Hydrographique et Océanographique de la Marine (SHOM) and Noveltis. We express our gratitude to Gurvan Madec and his team for having made their ocean model available. Fruitful discussions with Pierre Brasseur were particularly appreciated. Charles-Emmanuel Testut, Jean-Michel Brankart and Laurent Parent have developed powerful software that made the assimilation experiments and analysis so much easier. The plotting tools developed by Sébastien Masson were very helpful.

## References

Ando, K., and M. McPhaden, Variability of surface layer hydrography in the tropical Pacific Ocean, *J. Geophys. Res.*, *102*, 23,063–23,078, 1997.

Andreu Burillo, I., Etude d'impact de l'assimilation de la température de surfacce de la mer dans un modèle d'océan aux équations primitives: Application au cas SEMAPHORE, Ph.D. thesis, 199 pp., Univ. é Paul Sabatier, Toulouse, France, 2002.

Bell, M. J., M. J. Martin, and N. K. Nichols, Assimilation of data into an ocean model with systematic errors near the equator, *Ocean Appl. Tech. Note 27*, U.K. Met Off., Bracknell, 2001.

Blanke, B., and P. Delecluse, Variability of the tropical Atlantic Ocean simulated by a general circulation model with two different mixed layer physics, *J. Phys. Oceanogr.*, *23*, 1363–1388, 1993.

Bonjean, F., and G. Lagerloef, Diagnostic model and analysis of the surface currents in the tropical Pacific Ocean, *J. Phys. Oceanogr.*, *32*, 2938–2954, 2002.

Brasseur, P., J. Ballabrera, and J. Verron, Assimilation of altimetric data in the mid-latitude oceans using the Singular Evolutive Extended Kalman filter with an eddy-resolving, primitive equation model, *J. Mar. Syst.*, *22*, 269–294, 1999.

Burgers, G., M. A. Balmaseda, F. C. Vossepoel, G. J. van Oldenborgh, and P. J. van Leeuwen, Balanced ocean-data assimilation near the equator, *J. Phys. Oceanogr.*, *32*, 2509–2519, 2002.

Delcroix, T., and M. McPhaden, Interannual sea surface salinity and temperature changes in the western Pacific warm pool during 1992–2000, *J. Geophys. Res.*, *107*(C12), 8002, doi:10.1029/2001JC000862, 2002.

Delcroix, T., C. Hénin, V. Porte, and P. Arkin, Precipitation and sea surface salinity in the tropical Pacific Ocean, *J. Geophys. Res.*, *Part 1*, *43*, 1123–1141, 1996.

Delcroix, T., C. Hénin, F. Masia, and D. Varillon, *Three Decades of in Situ Sea Surface Salinity Measurements in the Tropical Pacific Ocean* [CD-ROM], Lab. d'Océanogr. Phys. du Cen. IRD de Nouméa, New Caledonia, 2000. (Available at http://www.ird.nc/ECOP.)

Delecluse, P., M. Davey, Y. Kitamura, S. Philander, M. Suarez, and L. Bengtsson, Coupled general circulation modeling of the tropical Pacific, *J. Geophys. Res.*, *103*, 14,357–14,376, 1998.

Deltel, C., Estimation de la circulation dans l'Atlantique Sud par assimilation variationnelle de données in situ, Ph.D. thesis, Lab. de Phys. des Océans, Brest, France, 2002.

Durand, F., L. Gourdeau, T. Delcroix, and J. Verron, Assimilation of sea surface salinity in a tropical OGCM: A twin experiment approach, *J. Geophys. Res.*, *107*(C12), 8004, doi:10.1029/2001JC000849, 2002.

Font, J., Y. Kerr, and M. Berger, Measuring ocean salinity from space, *Backscatter*, *11*, 17–19, 2000.

Fu, C., H. Diaz, and J. Fletcher, Characteristics of the response of sea surface temperature in the central Pacific associated with warm episodes of the Southern Oscillation, *Mon. Weather Rev.*, *144*, 1716–1738, 1986.

Fukumori, I., R. Raghunath, L. Fu, and Y. Chao, Assimilation of TOPEX/Poseidon altimeter data into a global ocean circulation model: How good are the results?, *J. Geophys. Res.*, *104*, 25,647–25,665, 1999.

Gibson, J. K., P. Kallberg, S. Upala, A. Nomura, A. Hernandez, and E. Serrano, ERA description, *ECMWF Re-Anal. Final Rep. Ser. 1*, 71 pp., Eur. Cent. for Med.-Range Weather Forecasts, Reading, U.K., 1997.

Gill, A. E., An estimation of sea level and surface current anomalies during the 972 El Niño and consequent thermal effects, *J. Phys. Oceanogr.*, *13*, 2148–2160, 1983.

GODAE International Project Office, The Global Ocean Data Assimilation Experiment Strategic Plan, *GODAE Rep. 6*, Melbourne, Victoria, Australia, 2000.

Gourdeau, L., J. Verron, T. Delcroix, A. J. Busalacchi, and R. Murtugudde, Assimilation of TOPEX/Poseidon altimetric data in a primitive equation model of the tropical Pacific Ocean, during the 1992–1996 ENSO period, *J. Geophys. Res.*, *105*, 8473–8488, 2000.

Hénin, C., and J. Grelet, A merchant ship thermosalinograph network in the tropical Pacific, *Deep Sea Res., Part I*, *43*, 1833–1855, 1996.

Kalnay, E., et al., The NCEP/NCAR 40-Year Reanalysis Project, *Bull. Am. Meteorol. Soc.*, *77*, 437–471, 1996.

Lagerloef, G., and T. Delcroix, Sea surface salinity: A regional case study for the tropical Pacific, in *Observing the Ocean in the 21st Century*, pp. 137–148, Aust. Bur. of Meteorol., Melbourne, Victoria, 2001.

Lengaigne, M., J.-P. Boulanger, C. Menkes, S. Masson, G. Madec, and P. Delecluse, Ocean response to the March 1997 Westerly Wind Event, *J. Geophys. Res.*, *107*(C12), 8015, doi:10.1029/2001JC000841, 2002.

Levitus, S., T. P. Boyer, and J. Antonov, *World Ocean Atlas*, vol. 5, *Interannual Variability of Upper Ocean Thermal Structure*, *NOAA Atlas NESDIS*, vol. 5, 176 pp., Natl. Oceanic and Atmos. Admin., Silver Spring, Md., 1994.

Lukas, R., and E. Lindstrom, The mixed layer in the western equatorial Pacific Ocean, *J. Geophys. Res.*, *96*, 3343–3358, 1991.

Madec, G., P. Delecluse, M. Imbard, and C. Levy, OPA 8.1 Ocean General Circulation Model reference manual, *Note Pole Modél. 11*, 91 pp., Inst. Pierre Simon Laplace, Paris, 1998.

Maes, C., M. J. McPhaden, and D. Behringer, Signatures of salinity variability in tropical Pacific Ocean dynamic height anomalies, *J. Geophys. Res.*, *107*(C11), 8012, doi:10.1029/2000JC000737, 2002.

McPhaden, M. J., Genesis and evolution of the 1997–1998 El Niño, *Science*, *283*, 950–954, 1999.

Menkes, C., J.-P. Boulanger, A. J. Busalacchi, J. Vialard, P. Delecluse, M. J. McPhaden, E. Hackert, and N. Grima, Impact of TAO vs. ERS wind stresses onto simulations of the tropical Pacific Ocean during the 1993–1998 period by the OPA OGCM, *Euroclivar Workshop Rep. 13*, pp. 46–48, Geneva, 1998.

Pham, D. T., J. Verron, and M. C. Roubaud, A singular evolutive extended Kalman filter for data assimilation in oceanography, *J. Mar. Syst.*, *16*, 323–340, 1998.

Picaut, J., and T. Delcroix, Equatorial wave sequence associated with the warm pool displacement during the 1986–1989 El Niño and La Niña, *J. Geophys. Res.*, *100*, 18,398–18,408, 1995.

Picaut, J., F. Masia, and Y. DuPenhoat, An advective-reflective conceptual model for the oscillatory nature of the ENSO, *Science*, *277*, 663–666, 1997.

Reynolds, D., and T. Smith, Improved global sea surface temperature analyses using optimum interpolation, *J. Clim.*, *7*, 929–948, 1994.

Reynolds, R. W., M. Ji, and A. Leetmaa, Use of salinity to improve ocean modeling, *Phys. Chem. Earth*, *23*, 543–553, 1998.

Roullet, G., and G. Madec, Salt conservation, free-surface and varying levels: A new formulation for an Ocean GCM, *J. Geophys. Res.*, *105*, 23,927–23,942, 2000.

Sprintall, J., and T. Tomczak, Evidence of the barrier layer in the surface layer of the tropics, *J. Geophys. Res.*, *97*, 7305–7316, 1992.

Stockdale, T., A. Busalacchi, D. Harrison, and R. Seager, Ocean modeling for ENSO, *J. Geophys. Res.*, *103*, 14,325–14,356, 1998.

Testut, C. E., P. Brasseur, J. M. Brankart, and J. Verron, Assimilation of sea-surface temperature and altimetric observations during 1992–1993 into an eddy permitting primitive equation model of the North Atlantic Ocean, *J. Mar. Syst.*, *40–41*, 291–316, 2003.

Vialard, J., and P. Delecluse, An OGCM study for the TOGA decade. part I: Role of salinity in the physics of the western Pacific fresh pool, *J. Phys. Oceanogr.*, *28*, 1071–1088, 1998.

Vialard, J., C. Menkes, J.-P. Boulanger, P. Delecluse, E. Guilyardi, M. J. McPhaden, and G. Madec, A model study of oceanic mechanisms affecting equatorial Pacific sea surface temperature during the 1997–98 El Niño, *J. Phys. Oceanogr.*, *31*, 1649–1675, 2001.

Vialard, J., P. Delecluse, and C. Menkes, A modeling study of salinity effects during the 1997–1998 El Niño, *J. Geophys. Res.*, *107*(C12), 8005, doi:10.1029/2000JC000758, 2002.

Weaver, A. T., J. Vialard, D. L. T. Anderson, and P. Delecluse, Three- and four-dimensional variational assimilation with a general circulation model of the tropical Pacific Ocean, *ECMWF Tech. Memo. 365*, Eur. Cent. for Med.-Range Weather Forecasts, Reading, 2002.

Xie, P., and P. Arkin, Analyses of global monthly precipitation using gauge observations, satellite estimates, and numerical model predictions, *J. Clim*, *9*, 840–858, 1996.

J. Verron, Laboratoire des Ecoulements Géophysiques et Industriels (LEGI), CNRS, B. P. 53X, 38041 Grenoble Cedex, France.

T. Delcroix, F. Durand, and L. Gourdeau, LEGOS, 14 Ave. E. Belin, 31401 Toulouse cedex 4, France. (lionel.gourdeau@cnes.fr)